Finite element modelling to assess the effect of surface mounted piezoelectric patch size on vibration response of a hybrid beam

N Rahman[1] **and M N Alam**[2]

[1,2] Department of Mechanical Engineering, Zakir Husain College of Engineering and Technology, A. M. U. Aligarh, Uttar Pradesh, India.

E-mail: [1]najeebalig@rediffmail.com,[2]naushad7863@rediffmail.com

Abstract. Vibration response analysis of a hybrid beam with surface mounted patch piezoelectric layer is presented in this work. A one dimensional finite element (1D-FE) model based on efficient layerwise (zigzag) theory is used for the analysis. The beam element has eight mechanical and a variable number of electrical degrees of freedom. The beams are also modelled in 2D-FE (ABAQUS) using a plane stress piezoelectric quadrilateral element for piezo layers and a plane stress quadrilateral element for the elastic layers of hybrid beams. Results are presented to assess the effect of size of piezoelectric patch layer on the free and forced vibration responses of thin and moderately thick beams under clamped-free and clamped-clamped configurations. The beams are subjected to unit step loading and harmonic loading to obtain the forced vibration responses. The vibration control using in phase actuation potential on piezoelectric patches is also studied. The 1D-FE results are compared with the 2D-FE results.

1. Introduction

Many light weight structural components are made of composite and sandwich laminates because of their high stiffness to weight ratio and similar other properties. Most of these components are generally modelled as smart multi-layered beams. These have found varied applications in the aerospace, robotics, defense equipments, measurement devices, satellites, automobile and ship building industries. Precise analysis of hybrid laminates require systematic and precise approximation of the displacement and the potential field across the thickness. Hodges et al. [1] presented methods for predicting the vibration frequencies of composite beams and their mode shapes. They proposed different methods to determine the sectional elastic constants and ways to solve the equations of motion. Banergee [2] used dynamic stiffness matrix method to carry out the free vibration analysis of composite Timoshenko beams loaded in axial direction. The theory includes the coupling between the bending and torsional modes of deformations. Lee et al. [3] used ESL theories for transient analysis of laminated structures. Kapuria et al. [4] developed an efficient coupled one-dimensional model for the dynamics of piezoelectric composite beams and presented a one-dimensional beam finite element with electric degrees of freedom [5]. A unified theory for smart beam with piezoelectric sensors and actuators is presented by Kapuria and Hagedorn [6]. Della and Shu [7] studied vibration of smart

---

[1]   To whom any correspondence should be addressed.

beams using micromechanics approach. Chevallier et al. [8] presented a 3D FE simulation for free vibration of thick beams and plates with a symmetric pair of surface mounted piezoceramic patches. Rahman and Alam [9-11] presented 1D-FE modelling using layerwise (zigzag) theory for dynamic analysis of smart laminated beam. Giunta et al. [12] studied free-vibration analysis of cross-ply beams under simply supported configuration. They used various higher-order and classical theories for the analysis and approximated the through the thickness displacement field in the form of a polynomial expansion. Koutsawa et al. [13] presented 1D finite elements to attain the free vibration response of composite smart beams. They approximated displacements and electric potential using Lagrange's polynomials. Shang et al. [14] used Generalized FE Method to carry out the dynamic analyses of 1D bar and beam problems. They compared their results with conventional FE formulation to prove efficiency of the method. Sayyad A S and Ghugal [15] presented a critical review of literature on bending, buckling and vibration analysis of laminated beams based on various theories. He et al. [16] proposed a new model for the two-layer composite beam with partial interaction by modifying Reddy's higher order beam theory. They used Hamilton's principle for formulation of governing equations for free vibration and buckling.

A one dimensional finite element (1D-FE) model based on efficient layerwise (zigzag) theory is presented for the vibration response analysis of a hybrid beam with surface mounted patch piezoelectric layers. The size of the piezoelectric patches are varied and its effects on free and forced vibration responses are studied. Results are presented for thin and moderately thick beams under clamped-free and clamped-clamped configurations. Unit step pressure loading and harmonic pressure loading are applied to set forced vibration in beam. The vibration control using in phase actuation potential on piezoelectric patches is also studied. The 1D-FE results are compared with the 2D-FE results.

2. Finite element model of hybrid beam with patch piezoelectric layers

Consider a hybrid beam with surface mounted piezoelectric patches. The beam is divided into elastic and hybrid segments due to the existence of these patches. Using coupled zigzag theory approximations [5], the potential and displacement field variables ϕ, u_x and u_z are assumed as

$$\phi(x,z,t) = \xi_\phi^l(z)\phi^l(x,t) \tag{1}$$

and

$$\begin{Bmatrix} u_x \\ u_z \end{Bmatrix} = \begin{bmatrix} g_1(z) & O_{1x2} \\ O_{1x4} & g_2(z) \end{bmatrix} \begin{Bmatrix} \tilde{u}_1 \\ \tilde{u}_2 \end{Bmatrix} \tag{2}$$

with

$$g_1(z) = \left\{ 1 \quad z \quad S^k(z) \quad S^{kl'}(z) \right\}, \ g_2(z) = \left\{ 1 \quad \bar{\xi}_\phi^{l'}(z) \right\} \tag{3}$$

$$\tilde{u}_1 = \left\{ u_{x_0} \quad -\frac{\partial u_{z_0}}{\partial x} \quad \psi_0 \quad \frac{\partial \phi^{l'}}{\partial x} \right\}^T, \ \tilde{u}_2 = \left\{ u_{z_0} \quad -\phi^{l'} \right\}^T \tag{4}$$

where $O_{1\times2}$ and $O_{1\times4}$ are null matrices of order 1x2 and 1x4 respectively; $\phi^l(x,t) = \phi(x,z_\phi^l,t)$; $\xi_\phi^l(z)$ are linear interpolation functions for ϕ; $\tilde{u}_1$ and $\tilde{u}_2$ are the generalised displacements; $\bar{\xi}_\phi^{l'}(z)$ is a piecewise linear function; $S^k(z), S^{kl'}(z)$ are the cubic functions of z. The indices l, l' take values $1, 2, ---, n_\phi$.

The assumed displacement field satisfies the continuity of u_x and σ_{zx} at the interfaces of layers and the shear traction-free state at the bottom surface and top surface of the beam. Using partially nonlinear strain-displacement relations and electric field-potential relations, the strains and electric fields are obtained as:

$$\left\{ \begin{array}{c} \varepsilon_x \\ \gamma_{zx} \end{array} \right\} = \left\{ \begin{array}{c} \dfrac{\partial u_x}{\partial x} + \dfrac{1}{2}\left(\dfrac{\partial u_{z0}}{\partial x}\right)^2 \\[2mm] \dfrac{\partial u_x}{\partial z} + \dfrac{\partial u_z}{\partial x} \end{array} \right\} = \left[\begin{array}{cc} g_1(z) & 0 \\ 0 & g_5(z) \end{array} \right] \left\{ \begin{array}{c} \tilde{\varepsilon}_1 \\ \tilde{\varepsilon}_5 \end{array} \right\} + \left\{ \begin{array}{c} \dfrac{1}{2}\left(\dfrac{\partial u_{z0}}{\partial x}\right)^2 \\ 0 \end{array} \right\} \tag{5}$$

$$\left\{ \begin{array}{c} E_x \\ E_z \end{array} \right\} = \left\{ \begin{array}{c} -\dfrac{\partial \phi}{\partial x} \\[2mm] -\dfrac{\partial \phi}{\partial z} \end{array} \right\} = \left\{ \begin{array}{c} E_x^{(1)} \\ E_z^{(1)} \end{array} \right\} \xi_\phi^{l'}(z) + \left\{ \begin{array}{c} E_x^{(2)} \\ E_z^{(2)} \end{array} \right\} \dfrac{\partial \xi_\phi^{l'}(z)}{\partial z} \tag{6}$$

where $\tilde{\varepsilon}_1$ and $\tilde{\varepsilon}_5$ are the generalised beam mechanical strains; $E_x^{(1)}, E_z^{(1)}$, $E_x^{(2)}$ and $E_z^{(2)}$ are the electric field components.

Let q_b be the pressure on the bottom surface and q_t on the top surface of the beam. The variational equation, using the extended Hamilton's principle [17] for the beam, is obtained as:

$$\int_0^a \left[\delta \tilde{u}_1^T I \ddot{\tilde{u}}_1 + \delta \tilde{u}_2^T \tilde{I} \ddot{\tilde{u}}_2 + \delta \tilde{\varepsilon}_1^T F_1 + \delta \tilde{\varepsilon}_5^T F_5 + \left\{ \dfrac{\partial \delta \phi^l}{\partial x} \quad \delta \phi^l \right\} \left\{ H^l \quad G^l \right\}^T \right.$$
$$\left. - \delta \tilde{u}_2^T \left\{ (q_2 + \hat{q}_2) \quad -(q_4^l + \hat{q}_4^l) \right\}^T + \left(\dfrac{\partial \delta u_{z_0}}{\partial x} N_x \dfrac{\partial u_{z_0}}{\partial x} \right) \right] dx$$
$$- \left[N_x^* \delta u_{x_0}^* + V_x^* \delta u_{z_0}^* - M_x^* \dfrac{\partial \delta u_{z_0}^*}{\partial x} + P_x^* \delta \psi_0^* + \left(H^{l*} - V_\phi^{l*} \right) \delta \phi^{l*} + R_x^{l*} \dfrac{\partial \delta \phi^{l*}}{\partial x} \right]_0^a = 0 \tag{7}$$

where $I, \tilde{I}$ are inertia matrices; $F_1 = \left\{ N_x \quad M_x \quad P_x \quad R_x^l \right\}^T , F_5 = \left\{ Q_x \quad \bar{Q}_x^l \right\}^T$ and V_x, V_ϕ^l are the beam stress resultants; H^l and G^l are the beam electric displacement resultants; q_2 is the mechanical load, q_4^l is the electrical load, $\hat{q}_2$ and $\hat{q}_4^l$ are the damping loads. The superscript * means values at the ends.

A two noded beam element is considered for making the finite element model. Each element has eight mechanical degrees of freedom and fluctuating number of electric degrees of freedom. The transverse deflection and electric potential are expanded using cubic Hermite interpolation functions. Axial displacement and shear rotation are expanded using linear Lagrange interpolation functions.

The element generalized displacement vector, d^e is defined as

$$d^{e^T} = \left\{ u_{x_0}^{e^T} \quad u_{z_0}^{e^T} \quad \psi_0^{e^T} \quad \phi^{l^{e^T}} \right\} \tag{8}$$

where $u_{x_0}^e, u_{z_0}^e, \psi_0^e, \phi^{l^e}$ are the nodal value vectors.

Considering terms for linear analysis only, the participation T^e of one element to the integral in equation (7) is attained as

$$T^e = \int_0^l \delta d^{e^T} \left[\bar{B}_m^T \bar{I} B_m \ddot{d}^e + \bar{B}^T \bar{D} \bar{B} d^e - \bar{B}_{m_2}^T g_{u\phi} + \bar{B}_2^T \bar{C}_2 \bar{B}_2 \dot{d}^e \right] dx$$
$$= \delta d^{e^T} \left[M^e \ddot{d}^e + C^e \dot{d}^e + K^e d^e - P^e \right] \tag{9}$$

where,

$\bar{I}$ is beam inertia matrix; $\bar{D}$ is the generalized stiffness matrix of the beam; $\bar{B}_{m_2}, \bar{B}_m, \bar{B}_2$ are displacement interpolation matrices and $\bar{B}$ is strain displacement interpolation matrix.

The contributions from all the elements are summed up to obtain the system equation as

$$M\ddot{d} + C\dot{d} + Kd = P \qquad (10)$$

where M, C and K are assembled from element inertia, damping and stiffness matrices M^e, C^e and K^e respectively. d, P are the assembled displacement and load vectors respectively.

Equation (10) can be partitioned and the damping matrix and load terms are set as zero to obtain the undamped free vibration response. The emanating eigenvalue problem is solved using subspace iteration method to acquire first n undamped natural frequencies ω_n.

3. Results and discussion

A composite substrate (b) and a sandwich substrate (c) are considered for the analysis. The substrate (b) is a symmetric graphite epoxy composite laminate of four layers with layup (0°/ 90°/90°/0°) and thicknesses ($0.25h$/$0.25h$/$0.25h$/$0.25h$). The substrate (c) is a symmetric sandwich laminate of three layers. The thickness of top and bottom face sheets is taken as $0.08h$ and the thickness of soft core is taken as $0.84h$. Here h is the total thickness of the elastic substrate for both the beams. Piezoelectric patch (PZT-5A) is bonded on top surface of the elastic substrate at fixed end for cantilever configuration and at one of the clamped ends for clamped-clamped configuration. The width of the beam and piezo patch are modelled as unity and the thickness of piezo-patches is taken as $0.1h$. The length of PZT-5A patch, l_p, is varied to assess the effect of variation in size of piezoelectric patch on the dynamic response of hybrid beam. The bottom and top surfaces of the elastic substrate are grounded. The results are obtained for span to thickness ratio, $S = l / h = 10, 20$. Here l is the length of beam. The properties of graphite epoxy composite lamina, the face, the core and the PZT-5A are taken from Ref. [10].

3.1. Free vibration response

The beams are modelled with $l_p = 0.2l, 0.4l, 0.6l, 0.8l, l$ and analysed for free vibration response for graphite epoxy composite substrate (b) and sandwich substrate (c).

Figure 1 shows the variation of normalised natural frequencies with mode of vibrations for beam b with varied piezo patch sizes. Results are plotted for first five vibration modes. The frequencies are non-dimensionalised as: $\bar{\omega}_n = \omega_n l S \, \rho_0^{1/2} / Y_0^{1/2}$.
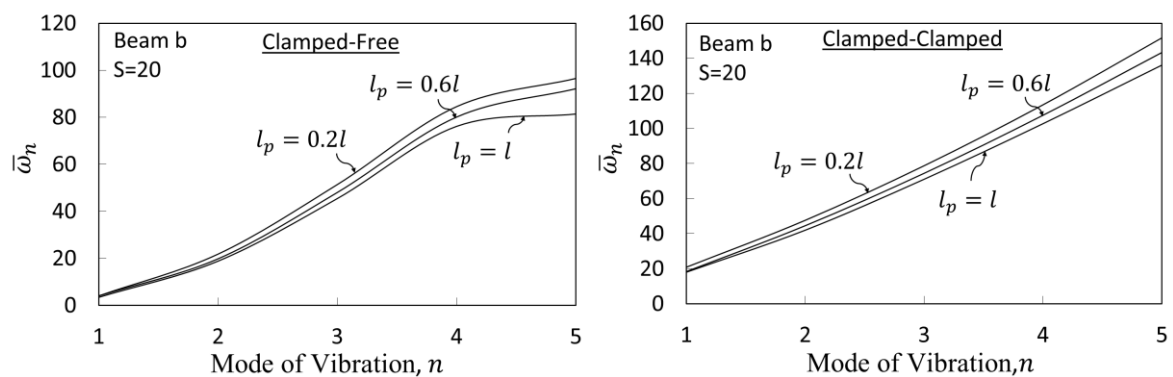

Figure 1. Variation of natural frequency with mode of vibrations for beam b with varied piezo-patch sizes.

For a given patch size the frequency increases with mode of vibration, n. With increase in size of piezo patch layer, the normalised natural frequencies decrease for all the vibration modes. Similar observations are obtained for beam c (figure 2). This decrease is less significant for lower modes ($n = 1, 2, 3$) but more significant for higher modes ($n = 4, 5$). The amount of decrease is more in

sandwich beam c in comparison to the composite beam b. For a given beam configuration the frequencies corresponding to clamped-clamped beam are higher in comparison to clamped-free beam.
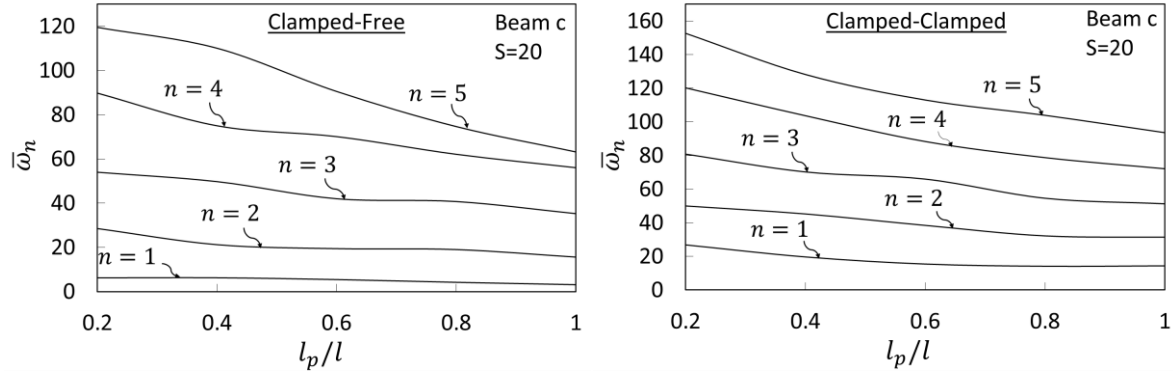

Figure 2. Variation of natural frequencies with size of piezo-patch layer for beam c.

Table 1. Comparison of natural frequencies for beam b.

S	l_p/l	Natural Frequency	Clamped-Free		Clamped-Clamped	
			1D-FE	2D-FE	1D-FE	2D-FE
	0.4	$\bar{\omega}_1$	3.81	3.81	14.14	13.83
		$\bar{\omega}_2$	15.75	15.43	29.22	28.40
10		$\bar{\omega}_3$	33.36	32.75	48.48	46.42
	0.8	$\bar{\omega}_1$	3.52	3.51	12.66	12.40
		$\bar{\omega}_2$	15.03	14.80	27.35	26.52
		$\bar{\omega}_3$	31.96	31.34	45.23	43.23
	0.4	$\bar{\omega}_1$	4.10	4.10	19.82	19.67
		$\bar{\omega}_2$	20.76	20.61	44.92	44.46
20		$\bar{\omega}_3$	48.48	48.21	77.28	75.75
	0.8	$\bar{\omega}_1$	3.79	3.79	17.75	17.59
		$\bar{\omega}_2$	19.84	19.72	42.15	41.51
		$\bar{\omega}_3$	46.82	46.40	72.62	70.91

Table 1 and table 2 show comparison of first three normalised natural frequencies for beam b and beam c respectively with different piezo patch sizes for span to thickness ratios, $S = 10, 20$. The values of frequencies increase as the beam becomes thinner for both the end conditions. The results are in compliance with the 2D-FE results obtained using ABAQUS for both the hybrid beams.

3.2. Forced vibration response
A uniform upward pressure load, $q_t = q_0 F(t)$, over entire beam length on the top surface of beam and in phase uniform potential, $\phi^{n\phi} = \phi_0 F(t)$ on top surface of piezo patch is applied to obtain the forced vibration response. The axial and transverse displacements (u_x, u_z), the normal stress (σ_x), the potential (ϕ) and time (t) are nondimensionalised as

$$\bar{u}_x = 100 u_x Y_0 / h S^3 q_0, \; \bar{u}_z = 100 u_z Y_0 / h S^4 q_0, \; \bar{\sigma}_x = \sigma_x / S^2 q_0, \; \bar{\phi} = 100 \phi Y_0 d_0 / h S^2 q_0, \; \bar{t} = t Y_0^{1/2} / \mu l \rho_0^{1/2}$$

For unit step loading, $F(t)=1$ and for harmonic loading, $F(t)=cos(20\pi\bar{t})$. The time history response of the tip displacement for undamped vibrating cantilever (clamped-free) beam are obtained for beam configurations b and c with varied piezo patch sizes. The results obtained using 1D-FE model are compared with the corresponding results obtained using 2D-FE model in figures 3 and 4. The applied actuation potential $\bar{\phi}_0$ is taken as $0, 20$ for harmonic loading and $0, 10$ for unit step loading. The time step is taken as 0.0006 sec. and time history is plotted for 1.2 sec.

Table 2. Comparison of natural frequencies for beam c.

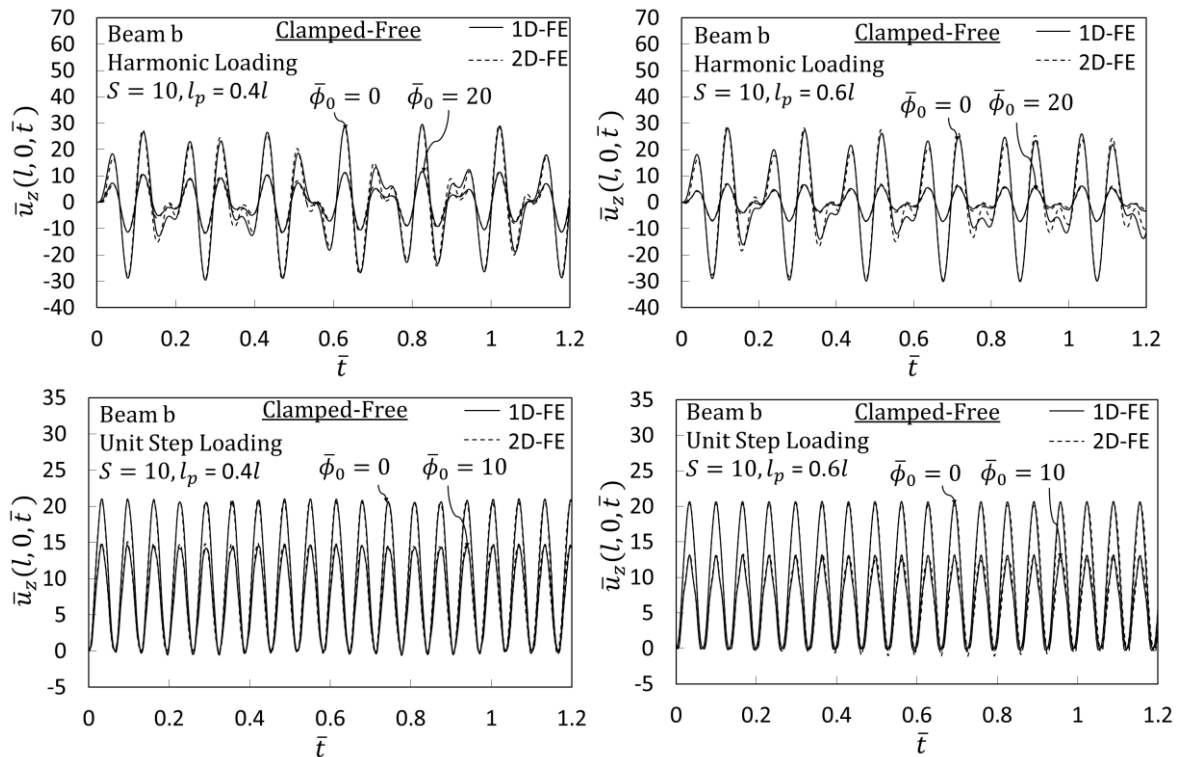| S	l_p/l	Natural Frequency	Clamped-Free 1D-FE	Clamped-Free 2D-FE	Clamped-Clamped 1D-FE	Clamped-Clamped 2D-FE
10	0.4	$\bar{\omega}_1$	5.37	5.37	12.35	12.12
		$\bar{\omega}_2$	14.17	13.91	27.21	26.62
		$\bar{\omega}_3$	31.89	30.92	40.55	38.93
	0.8	$\bar{\omega}_1$	3.57	3.55	8.94	8.74
		$\bar{\omega}_2$	12.80	12.56	19.04	18.52
		$\bar{\omega}_3$	25.27	24.71	31.30	30.12
20	0.4	$\bar{\omega}_1$	6.26	6.26	19.66	19.44
		$\bar{\omega}_2$	21.23	20.98	45.24	44.63
		$\bar{\omega}_3$	49.74	49.10	70.22	68.77
	0.8	$\bar{\omega}_1$	4.21	4.20	14.12	13.93
		$\bar{\omega}_2$	19.02	18.79	32.18	31.56
		$\bar{\omega}_3$	40.74	40.13	54.57	53.19

Figure 3. Time history of tip displacement for beam b.

The beams vibrate at the first natural frequency in case of unit step loading and at the forcing frequency in case of harmonic loading. It is observed that the size of piezo-patch layer has no significant effect on amplitude of vibration for closed circuit condition i.e. for $\bar{\phi}_0 = 0$. The controlled tip deflection is obtained with applied in phase actuation potential on top surface of piezo-patch layer and the amplitude of deflection can be minimised by using suitable value of the actuation potential. Further for the same actuation potential, the deflection amplitude can be restricted to a lower value with a larger size of piezo patch layer.
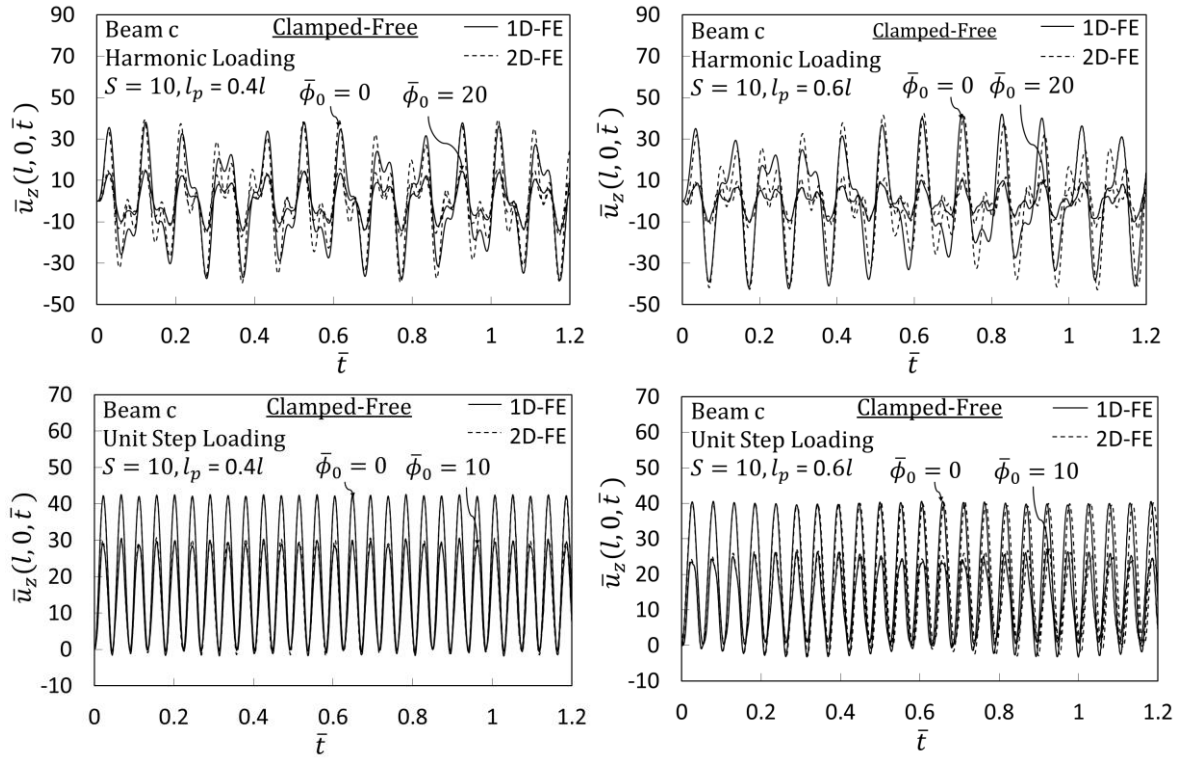

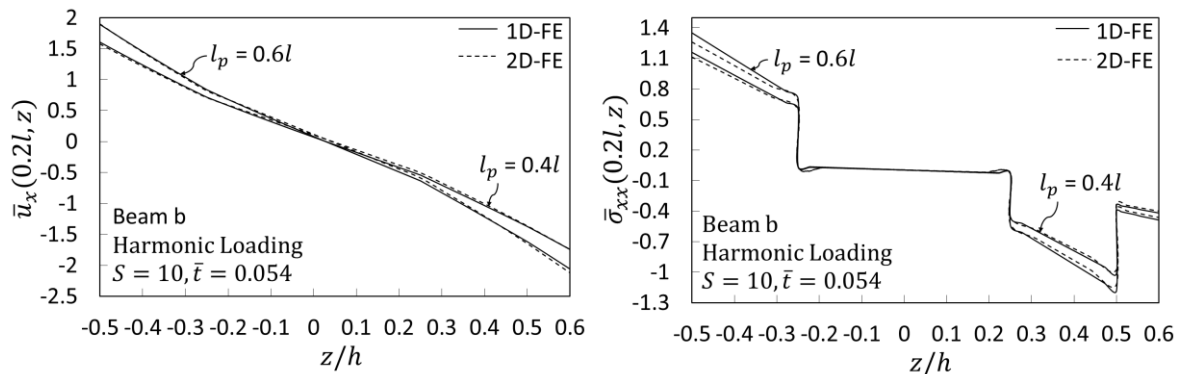**Figure 4.** Time history of tip displacement for beam c.

Figure 5. Comparison of through the thickness distribution of $\bar{u}_x$ and $\bar{\sigma}_{xx}$ for beam b.
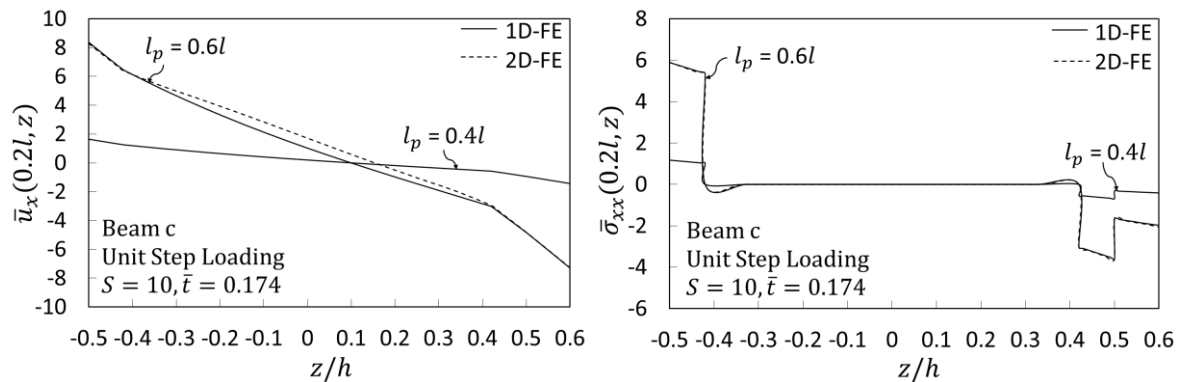
Figure 6. Comparison of through the thickness distribution of $\bar{u}_x$ and $\bar{\sigma}_{xx}$ for beam c.

Figures 5 and 6 show the comparison of distribution of axial displacement $\bar{u}_x$ and stress $\bar{\sigma}_{xx}$ across the beam thickness at $x = 0.2l$. The distribution is plotted at time, $\bar{t} = 0.054$ for beam b and $\bar{t} = 0.174$ for beam c with different sizes of piezoelectric patch layer. The 1D-FE distribution matches well with the 2D-FE distribution.

4. Conclusions

The size of piezoelectric patch layers in smart beams is significant as it results in different structural response. A 1D-FE model to assess the effect of size of piezoelectric patch layer on vibration response of a hybrid beam is presented. The results are obtained for clamped-free and clamped-clamped end conditions. With increase in size of piezo patch layer, the free vibration frequencies decrease for all the vibration modes. This decrease is less significant for lower modes but more significant for higher modes. In case of forced vibrations, the size of piezo-patch layer has no significant effect on amplitude of vibration for closed circuit condition i.e. for $\bar{\phi}_0 = 0$. The controlled tip deflection is obtained with applied in phase actuation potential on top surface of piezo-patch layer. The piezoelectric patch actuators of large size placed nearer to the fixed end with the application of appropriate actuation potential results in better control of tip deflection in cantilever beams. These observations may be used as a basis for experimental investigation and design for vibration control system for composite and sandwich hybrid structures.

5. References

[1]   Hodges D H, Atilgan A R, Fulton M V and Rehfield L W 1991 Free-vibration analysis of composite beams *J Am Helicop Soc*. **36** 36–47

[2]   Banerjee J R 1998 Free vibration of axially loaded composite Timoshenko beams using the dynamic stiffness matrix method *Computers & Structures* **69** 197–208

[3]   Lee S J, Reddy J N and Rostam-Abadi F 2004 Transient analysis of laminated composite plates with embedded smart-material layers *Finite Elem. Anal. Des.* **40** 463–483

[4]   Kapuria S, Dumir P C and Ahmed A 2003 An efficient coupled layerwise theory for dynamic analysis of piezoelectric composite beams *Journal of Sound and Vibration* **261** 927-944

[5]   Kapuria S and Alam N 2006 Efficient layerwise finite element model for dynamic analysis of laminated piezoelectric beams *Computer Methods in Applied Mechanics and Engineering* **195** 2742-2760

[6]   Kapuria S and Hagedorn P 2007 Unified efficient layerwise theory for smart beams with segmented extension/shear mode, piezoelectric actuators and sensors *Journal of Mechanics of Materials and Structures* **2** 1267-1298

[7]   Della CN and Shu D 2006 Vibration of beams with embedded piezoelectric sensors and actuators *Smart Materials and Structures* **15** 529–537

[8]   Chevallier G, Ghorbel S, Benjeddou A 2008 A benchmark for free vibration and effective coupling of thick piezoelectric smart structures *Smart Materials and Structures* **17** 065007/1–11

[9]   Rahman N and Alam M N 2014 Effect of thickness of piezoelectric layer on dynamic parameters of a laminated composite beam *Proc. of the Int. Mechanical Engineering Congress (IMEC, NIT-Trichy)* pp 319-323

[10]   Rahman N and Alam M N 2012 Dynamic analysis of laminated smart beams using zigzag theory *International Journal of Mechanics Structural* **3** 35-46

[11]   Rahman N and Alam M N 2010 Active vibration suppression of smart laminated cantilever beam using efficient zigzag theory *Proc. of the Nat. Conf. on Advances in Mechanical Engineering (NCAME-2010, A. M. U. Aligarh)* pp.241-248

[12]   Giunta G, Biscani F, Belouettar S 2013 Free vibration analysis of composite beams via refined theories *Composite Part B: Engineering* **44** 540–552

[13]   Koutsawa Y, Giunta G, Belouettar S 2014 A free vibration analysis of piezo-electric beams via hierarchical one-dimensional finite elements *Journal of Intelligent Systems and Structures* **25** 1009–1023

[14]   Shang H Y, Machado R D and Abdalla Filho J E 2016 Dynamic analysis of Euler–Bernoulli beam problems using the Generalized Finite Element Method *Computers and Structures* **173** 109–122

[15]   Sayyad A S and Ghugal Y M 2017 Bending, buckling and free vibration of laminated composite and sandwich beams: A critical review of literature *Composite Structures* **171** 486-504

[16]   He G, Wang D and Yang X 2016 Analytical solutions for free vibration and buckling of composite beams using a higher order beam theory *Acta Mechanica Solida Sinica*, **29** 300–315

[17]   H.F Tiersten 1969 *Linear Piezoelectric Plate Vibrations* (New York: Plenum Publishing Corporation)